Membrane Technology
ISSN (online): 1873-4049

Dynamic Analysis of Drill String and Wellbore in Ultra Short Radius Wells Based on Abaqus

Jiyong Che[1], Zhengwu Qiao[1,2*], Lei Chen[1], Mingna Li[1]
[1]*Federal Lanpec Technologies Limited, Lanzhou 730070, China*
[2]*Lanzhou Petroleum Machinery Research Institute Co., Ltd, Lanzhou 730070, China*
**Corresponding Author.*

Abstract:
Economic and efficient ultra-short radius horizontal drilling technology is an effective technology to increase the production of old oilfields. However, the fatigue breakage of the drilling string and wellbore and the coupling vibration between the drilling string and wellbore are the critical problems encountered in its engineering applications. We took the drilling string and wellbore of an experimental simulation of ultra-short radius as the object of research, set up the mechanical and mathematical model with strong adaptability, and applied theories to analyze the force condition of the drilling string and ultra-short radius wellbore. Consequently, a 3D computational model representing the drilling string and wellbore was built. The dynamic simulation software Abaqus was utilized to simulate the working force state of the ultra-short radius wellbore and drilling string, analyze the force generated by mutual contact movement under various operating conditions, and investigate the drilling string's dynamics and stability during the tripping process. The results reveal that the drill string's rotating speed influences its tripping ability: more intense the speed, greater the decrease in axial force. Thus, the rotational speed can be changed, and the lubrication between the wellbore and drill string can be improved to reduce the force between the drill string and wellbore, which is conducive to the entry of the drill string.

Keywords: ultra-short radius well; drill string passability; friction modeling; abaqus; kinetic analysis.

INTRODUCTION

Oil is an extremely important strategic resource of the country, the stone of our country Oil resources are generally distributed in rift basins as well as sedimentary basins at sea in the midst of the earth[1]. The complex distribution of geological environment leads to drilling in oil extraction Wells become one of the key jobs, and oilfield drilling is the development of petroleum energy The efficiency of the operation determines the smoothness of the entire development process Positive or not.

Horizontal well technology, which has promoted the rapid development of drilling technology, is a major breakthrough in the oil exploration industry. However, owing to the harsh drilling environment and complicated working conditions, especially in ultrashort-radius wells, fatigue breakage of the drill string and wellbore and coupled oscillation of the drill string and wellbore may easily occur and cause safety accidents. In ultra-short radius well research, the main focus is on the modelling and dynamics of the frictional resistance and frictional torque between the drill string and wellbore. In 1984, Johancsik [2] proposed a soft rod model to calculate the predicted frictional torque of a drilling string in directional wells. Huashan [3] used the large deformation theory to establish a rigid rod model, which assumes that the drill string is coincident with the borehole axis and considers the bending stiffness of the drill string. However, the equations of the model are more complicated and difficult to solve, and the calculation speed is slow, so it was not widely promoted. Gao et al. [4] used an mathematical technique to analyze the buckling behavior of a pressure-twist weightless string and concluded that the buckling configuration of a string subjected to a pressure-twist combination was an accurate helix. In terms of dynamics, Yang [5] studied the influence of drilling pressure, revolving velocity, and other factors on the three-dimensional (lengthways, lateral, and torsional) coupled vibration of a drilling string in an extended-reach horizontal well. Fan studied the cause of the fracture of the sprocket drive shaft of an oil drilling winch, and proposed to change the radius of the shaft diameter and reducer area. Wang [6] used ANSYS software to analyze the tripability of a drilling string in different cases. The stress state of the wellbore was mainly influenced by the simultaneous bending and tensile stresses. However, the contact stress was small. Existing models for calculating frictional resistance and frictional torque are divided into two main categories: soft rod and rigid rod models [7-11], which have their own assumptions and applicable conditions. Most models ignore the influence of many factors, such as the dynamics of the string. Hence, the calculation results have a certain degree of deviation from the actual situation. However, there are many factors that influence the formation of damage and destabilization of the drill string and wellbore during the actual tripping process, and the coupling between these factors is not clear, especially in the study of ultra-short radius wells, which is more complicated. In this study, we consider a model experimental well of ultra-short radius of "9-5/8" specification (bending radius 27 m, curvature 63. 7/30 m) as the object of study. We plan to study the force and damage mechanism of the drilling string and wellbore under different working conditions by developing a force mathematical model, conducting dynamics simulations, and taking into account all of the primary variables

in the actual operation of the drilling string. This will serve as a reference for improving operational stability and structural optimization of ultra-short radius wells in practical engineering applications.

Establishment of Friction Model for Ultra-Short Radius Experimental Wells

The model experimental well with an ultra-short radius of 9-5/8 (bending radius of 27 m and curvature of 63. 7/30 m) mainly consists of three parts: oblique straight section, bending section, and horizontal section, as shown in Figure 1.

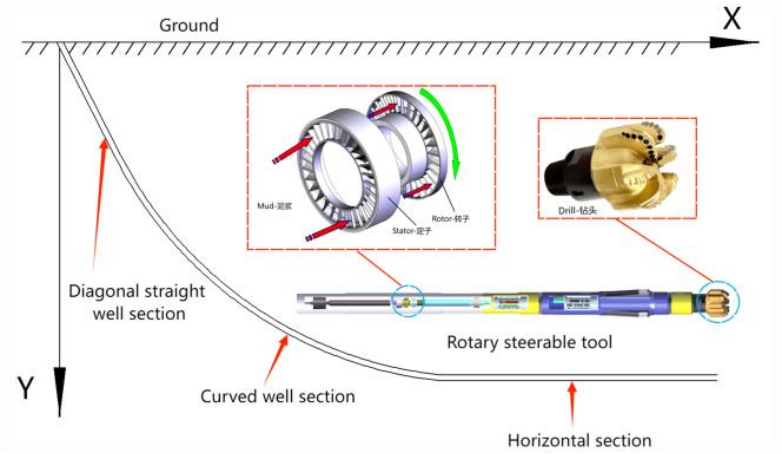

Figure 1. Ultra-short radius experimental well and drilling equipment

The drill string system moved axially along the trajectory of the wellbore, which was narrow and filled. However, it rotated under torque. In the annular space between the drill string and wellbore, there will also be "vortex motion" due to the centrifugal force. The actual operating conditions of ultra-short-radius downhole operations are relatively complex [12], and the drill string and wellbore are subjected to tension, pressure, bending, twisting, and the combined effects of complex loads, such as shear. Additionally, the smaller the curvature radius of the wellbore and longer the horizontal distance, the greater the frictional resistance of the string. This increased friction may hinder the drilling process and prevent the drill from smoothly reaching the bottom of the well. Nevertheless, it is unreasonable to consider all these in a single model. Only the main contradictions must be considered, and some secondary factors should be discarded. Consequently, the following presumptions were established: The drill string and wellbore's cross sections stayed circular, and the diameter did not vary when under load.

(1) The cross-section of the solar thermal power generation drill string and wellbore remains circular and the diameter remains unchanged under the action of load.

(2) The temperature changes in the wellbore and drill string due to energy changes were neglected.

(3) The material and size of the drill string do not need to be the same everywhere. However, they should remain unchanged locally.

(4) Initially, the trajectory of the drill string axis coincides with that of the wellbore.

Thus, the following is the fundamental concept for creating the model. The total axial force operating on the drill string system is equal to the sum of the axial forces acting on every single part of the drill string since the drill string system is made up of several segments of connected drill strings. Specifically, the direction was reversed and the axial force at the higher end of the lower drill string was equal to the axial force at the lower end of the upper drill string. The wellhead can be computed using this segmented computation approach. Moreover, the frictional force acting on the drill string system was equal to the sum of the frictional forces acting on each section. Finally, the frictional torque received was equal to the sum of the frictional torque received by the drill bit and frictional torque of each segment.

Establishment of oblique straight segment model

The gravity force per unit length of the drill string in the drilling fluid is defined as g_m, the coefficient of friction between the drill string and wellbore wall is marked as f, the diameter of the drill string is denoted as d_0, the unit length of the drill string is marked as Δ_L, the axial force applied to the lower end of this micrometric segment is T_0, and the force applied to the diagonal micrometric segment is shown in Figure 2.

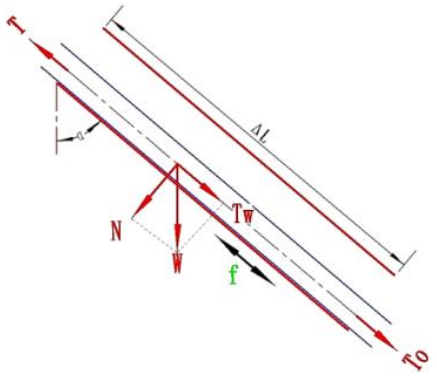

Figure 2. Schematic diagram of force on the inclined straight section

The gravity of the micro element drill string is $W=g_m \cdot \Delta_L$, axial component is $T_W = W \cdot \cos a$, and radial component is $N=W \cdot \sin a$. Then, the friction force is:

$$f_m = N \cdot f = W \cdot \sin \alpha \cdot f \tag{1}$$

When drilling up, f_m and T_W are in the same direction, and opposite when drilling down.

The axial force at the upper end is:

$$T = q_m \cdot \Delta L(\cos \alpha \pm f \cdot \sin \alpha) + T_0 \tag{2}$$

Consider "+" when drilling up and "−" when drilling down.

The slanting straight section mooring torque is:

$$= \frac{1}{2} q_m \cdot d_0 \cdot f \cdot \Delta L \cdot \sin \alpha \tag{3}$$

Modeling of curved segments

The drilling column and the wellbore in the curved section can make connection in three different ways: either the drilling column meets the upper wellbore wall in the fully curved section, the drilling column meets the lower wellbore wall in the fully curved section, or the drilling column meets the upper wellbore wall in the upper portion of the drilling column and the lower wellbore wall in the lower portion of the drilling column. There is also a point P that is just out of contact with the wellbore. Figure 3 displays the curved section's contact modes.

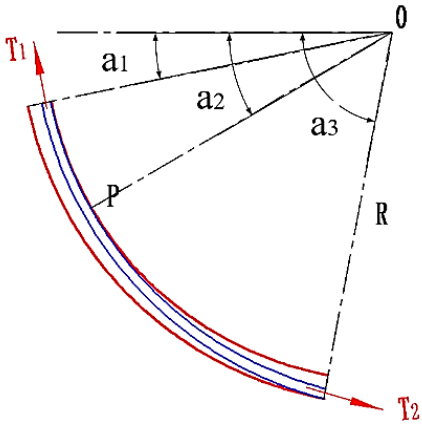

Figure 3. Schematic diagram of the contact pattern of the bending section

The force analysis models of different contact modes are different, and the forces received during the starting and lowering process will also be different. Taking micrometric segments d_L, the angle of the arc corresponding to it is d_α. The forces on the drill string in contact with the upper and lower well walls and when starting and stopping the drill are shown in Figure 4.

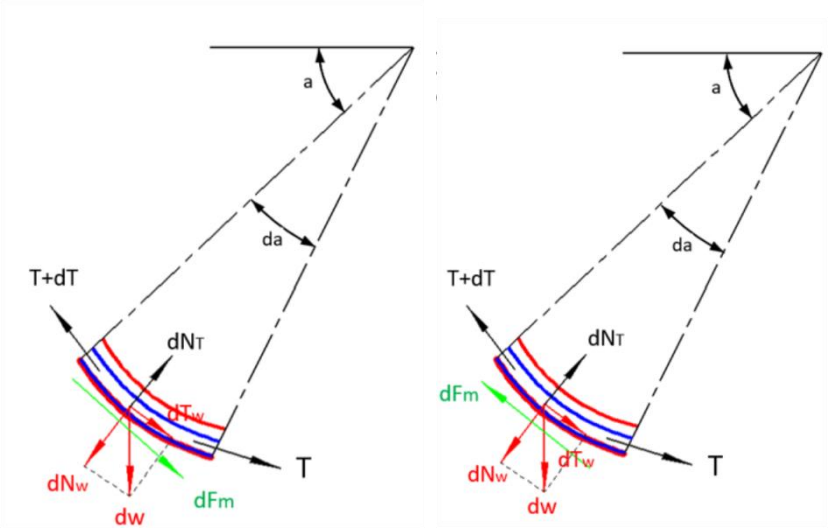

(a) Drill up, downhole wall contact (b) Drilling down, downhole wall contact

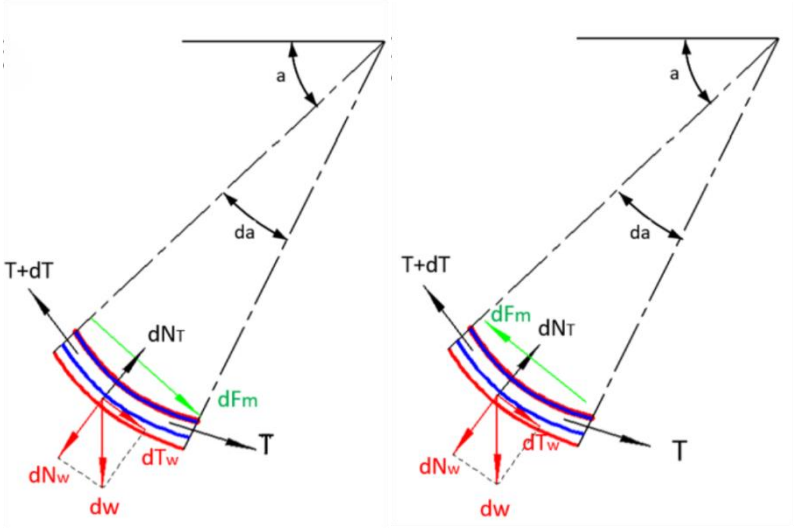

(c) Drill up, upper well wall contact (d) Drilling down, downhole wall contact

Figure 4. A schematic illustration of the contact force between the microelement drilling column and the curved well wall

Figure 4 shows the differential equation for the contact between the drill string and the downhole wall.

$$\frac{dT}{d\alpha} \mp T\,f = -q_m R(\cos\alpha \pm f\sin\alpha) \tag{4}$$

The same process is used to generate the differential equation for the drill string's contact with the upper well wall:

$$\frac{dT}{d\alpha} \pm T\,f = -q_m R(\cos\alpha \mp f\sin\alpha) \tag{5}$$

The drill was started with the symbol at the top and the bottom drill at the bottom.

Solving Eqs. (4) and (5) yields the upper-end tension force:

$$T_1 = T_2 \cdot e^{-(\alpha_2-\alpha_1)} + \frac{q_m R}{1+f^2}\left[\begin{array}{l}(1-f^2)(\sin\alpha_2 \cdot e^{-f(\alpha_2-\alpha_1)} - \sin\alpha_1) \\ -2(\cos\alpha_2 \cdot e^{-f(\alpha_2-\alpha_1)} - \cos\alpha_1)\end{array}\right] \tag{6}$$

$$\text{Let } S = \frac{q_m R}{1+f^2}\left[\begin{array}{l}(1-f^2)(\sin\alpha_2 \cdot e^{-f(\alpha_2-\alpha_1)} - \sin\alpha_1) - \\ 2(\cos\alpha_2 \cdot e^{-f(\alpha_2-\alpha_1)} - \cos\alpha_1)\end{array}\right], \; Q = e^{-(\alpha_2-\alpha_1)}.$$

Eq. (6) must consider the positivity and negativity of the friction coefficient f. Details of the selection process are presented in Table 1.

Table 1. Directional provisions for friction coefficient f under different operating conditions

Exposure/working conditions	Contact with downhole wall	Contact with upper well wall
Drill up	+	-
Drilling down	-	+

The contact state in the well section is affected by positive pressures caused by gravity (centrifugal direction) and axial tension (centripetal direction), and the key lies in the size of T_2. When T_2increases, the drill string tends to contact the upper well wall. When T_2 increases to a certain extent and exceeds the critical value will appear the whole section contact with the upper well wall. Contrariwise, as T_2 decreases, the drill string tends to contact the downhole wall, and when T_2 decreases to a certain extent and is less than the critical value T_{2x}, a situation of full section contact with the downhole wall will occur. Therefore, when $T_2 \ll T_{2x}$, the drill string comes into contact with the wellbore wall. When $T_2 \gg T_{2s}$, the drill string comes into contact with the upper wellbore wall. When $T_{2x}<T_2<T_{2s}$, There is a point P that just so happens to be out of touch with the wellbore, and the contact condition connecting the drill string and the wellbore is of the third type.

For the third contact state, it is necessary to calculate point P:

$$Q=e^{f(\alpha_p-\alpha_2)}$$

$$S=\frac{q_m R}{1+f^2}\left[\begin{matrix}(1-f^2)(Q\sin\alpha_2-\sin\alpha_p)\\ 2f(Q\cos\alpha_2-\cos\alpha_p)\end{matrix}\right]$$

$$\text{where } \sin\alpha_p=\frac{T_2\cdot Q+S}{q_m R} \text{ and } T_p=T_2Q+S. \tag{7}$$

By solving the above equations, the axial force T_p at point P and the corresponding well inclination angle α_p can be calculated according to the "contact with the upper well wall" for the part above point P. The part below point P is calculated according to the "contact with the lower well wall." The resistance and torsion in the curved section were obtained using Eq. 8.

$$M=q_m R f d_0(\cos\alpha_1-\cos\alpha_2)+\frac{1}{2}f d_0(\alpha_2-\alpha_1)(T_2+q_m R\sin\alpha_2) \tag{8}$$

where f is taken in the same direction as in Table 1.

ABAQUS FINITE ELEMENT DYNAMICS CALCULATIONS

Finite Element Modeling and Meshing

Shanghai Lanpec Technologies Limited created an ultra-short radius test well experimental system in response to research demands. The inclined-straight segment measured 14.145 m in length, the curved portion's arc length was 23.61 m, the horizontal section measured 19.215 mm, the curved segment's bending radius was 27 m, and its curvature was 63. 7°/30 m, as seen in Figure 5. In the tangential direction, the curved part neatly changed into two straight pieces.

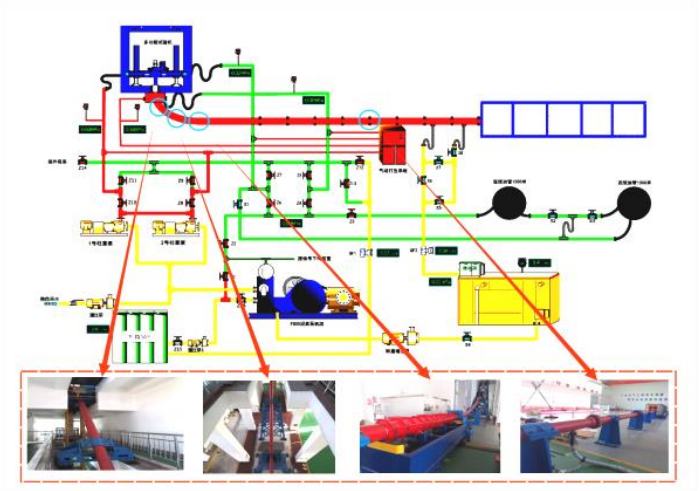

Figure 5. Experimental system for ultra-short radius test wells

The drill string and wellbore were modeled using the CREO software, and the wellbore and drill string's constructed three-dimensional model was imported into the Abaqus software for mesh division. The two components were meshed using the sweeping method. Considering the accuracy of the displacement and deformation solution results, an 8-node C3D8R hexahedral mesh was selected as the mesh type. To ensure that the mesh could accurately describe the calculated target force situation, the mesh was refined in the contact area. The finite element model and mesh are shown in Figure 6.

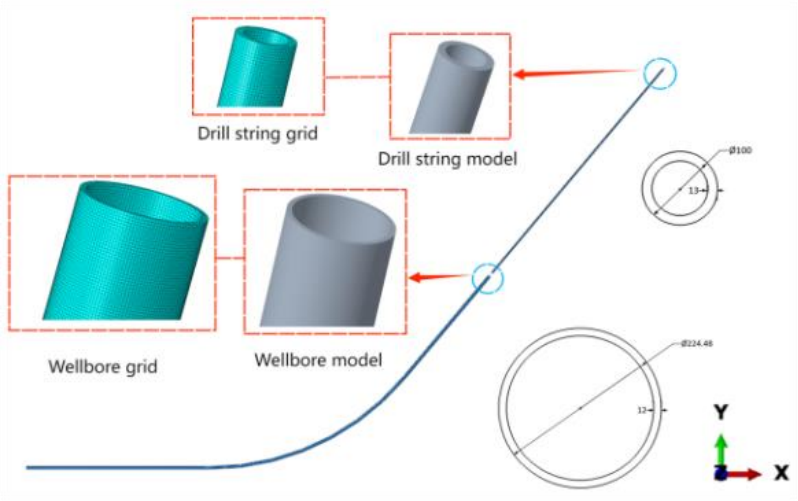

Figure 6. Finite element model and mesh division of drill string and wellbore

Abaqus Pre-Processing

ABAQUS is used to analyze and process complex solid and structural mechanical systems. Its implicit dynamics method does not require time integration, but is solved step-by-step through iteration. Although solving nonlinear equations has convergence issues, Abaqus uses the Newmark method, which can set larger time-increment steps. In the Abaqus/standard module, the Newton-Raphson algorithm is used to solve the nonlinear equations. When solving nonlinear problems, iterative balance control is mainly achieved through a semi-incremental step residual, which has obvious advantages in solving implicit dynamic problems [13]. The dynamic equation for the drill string system can be expressed as follows:

$$[M]\{\ddot{u}\}+[C]\{\dot{u}\}+[K]\{u\}=\{F(t)\} \tag{9}$$

where where the time-varying load function is denoted by F(t), the mass matrix is denoted by [M], the damping matrix by [C], the stiffness matrix by [K], and so on. The node acceleration, velocity, and displacement vectors are denoted by the letters "u"¨, "u", and "u" correspondingly. Figure 7 illustrates this following the application of the drill string and wellbore loads and limits.

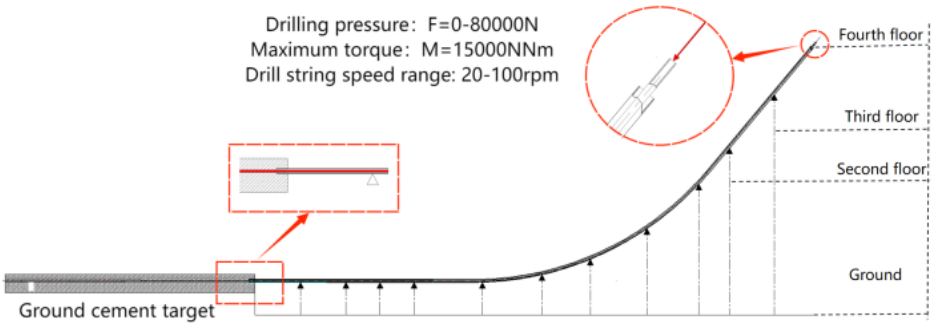

Figure 7. After application of drill string and wellbore loads and restraints

Before calculation, the model was processed and imported into Abaqus software [14]. The drill string and wellbore are assembled at the initial position in the assembly module, the material properties are defined in the property module, and they are assigned to the corresponding components. All the materials were defined as linear elastic materials, and their material properties are listed in Table 2.

Table 2. Material properties of drill string and wellbore

	Titanium alloy drill string		Ordinary drill string		Wellbore	
Mass Density (10^3 kg/mm^3)	4. 5E-009		7. 85E-009		7. 85E-009	
Young's modulus	113,200		200,000		200,000	
Poisson's ratio	0. 34		0. 3		0. 3	
Plasticity	860	0	860	0	758	0
	870	0. 001	870	0. 001	800	0. 005
	880	0. 005	880	0. 005	830	0. 015
	900	0. 010	900	0. 010	862	0. 025
	920	0. 020	920	0. 020		
	950	0. 035	950	0. 035		

The type of contact between the outer surface of the drill string and outer surface of the wellbore is defined as a surface-to-surface contact, with friction coefficients set to be 0. 2 and 0. 25, and mechanical constraint formulas using the penalty function method. The outer surface of the wellbore was fully fixed, and a load of 0-80,000 N drilling pressure was applied to the drill string with a rotation speed range of 20-100 r/min.

Calculation Results and Analysis

Passage analysis of the curved sections of the drill string

A force perpendicular to the drill string's cross-section was applied at the top of the string during the calculation process. The drill string's downward speed was set at 1 m/min in order to examine the effects of different factors on the drill string's downward movement. The drill string is first lowered into the wellbore, and once it has been lowered to a predefined point, the rotating speed is applied to the top of the drill string [14-17]. Figure 8 displays the results of the axial force in various modes and at various rotational speeds after the drill string is set to rotary drilling and lifting up.

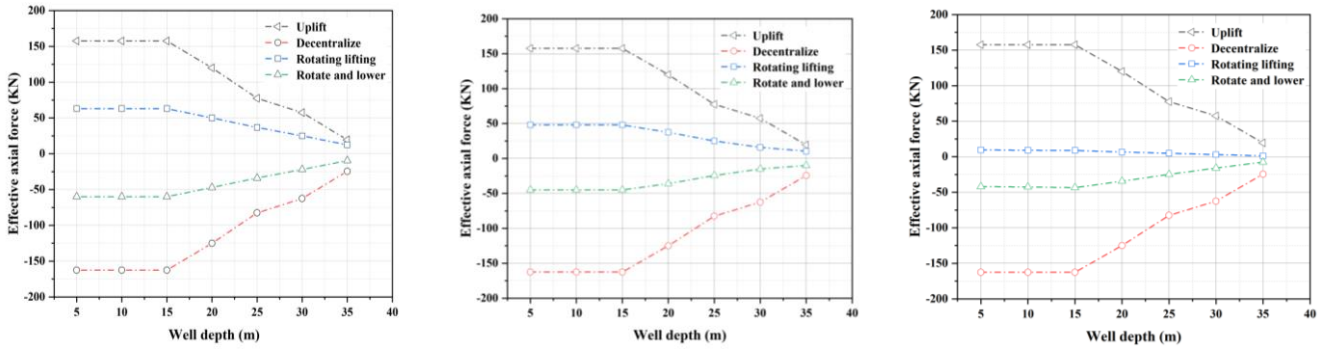

(a) n=20rpm (b) n=70rpm (c) n=100rpm

Figure 8. Comparison of effective axial force under different passing methods

From Figure 8, we can see that the sliding downthrust force is approximately 163. 8 KN, and the sliding uplift force is 166. 7 KN. The equipment capacity is sufficient to ensure that the drill column passes through the bending section smoothly. The drill column will be flexed when sliding down, but the influence on the drill column to pass through the bending section is relatively small. After adding the rotational speed, there is a significant reduction in the effective axial force, and the larger the rotational speed, the greater the degree of reduction of the axial force. The axial force decreases by 85. 6% when the rotational speed is. When the rotational speed is 100 rpm, the maximum axial force of rotary uplift is 9. 6 KN [18,19]. Compared with the rotary uplift force at 20 rpm, the force decreased by 85. 2%, which is due to the low axial velocity of the drilling column when rotating down or due to rotary uplift. This shows that the rotation can significantly reduce the friction of the drilling column.

Drill string friction torque analysis

Under the premise of maintaining a rotation speed of 70 rpm, different friction coefficients were set, and the change in the drill string friction torque was calculated. The results are presented in Figure 9.

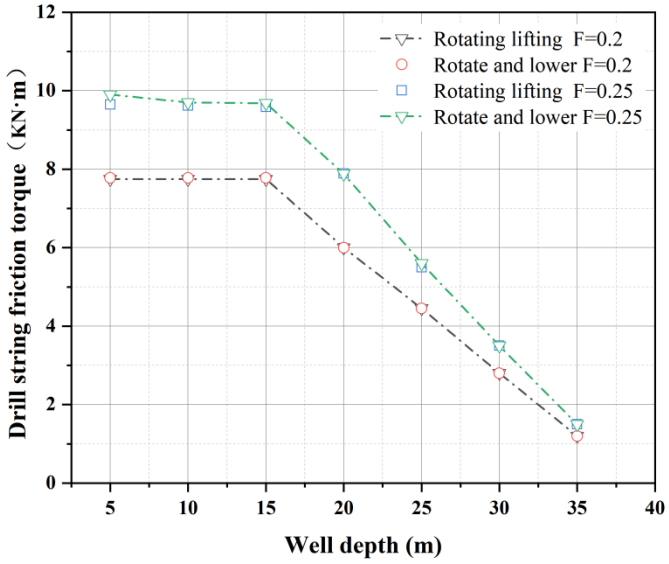

Figure 9. Comparison of the friction torque of the drill string at 70 rpm

From Figure 9, we can observe that the influence of the horizontal section on the friction torque is small, and the difference in friction torque between rotating up and rotating down under the same friction coefficient is small, at a maximum of 2. 5%. When rotating the drilling column through the wellbore, the different friction coefficients f corresponds to different torques of the drilling column. The torque of the column is smaller than 8 KN·m when f is 0. 2. The torque of the column is smaller than 10 KN·m when f is 0. 25. During the process of rotation, the axial friction is small, and the drilling column of the inclined straight section may exhibit slight spiral buckling [20,21]. To improve the force situation of the drill column and facilitate the lowering of the drill column, measures can be taken, such as rotating the drill column to improve the lubrication between the drill column

RESULTS

When the rotational speed was 100 rpm, the highest achievable axial force of the rotary lifting was 9.6 KN, which was 85.2% less than at 20 rpm. At high revolving speeds, the drill string's axial speed was slow, and the rotary-lifting force was greatly reduced. The parallel segment has very little impact upon the drill string's friction and torsion. The drill string in the oblique straight segment may display small spiral buckling while rotating through, and the friction torque of the drill string varies little at the same velocity and friction coefficient.

CONCLUSION

The disadvantage of this study is that there are few studies on the friction between the drill string and the wellbore, and it is difficult to study the lubricity between the two. Drilling tools are an important mechanical group for drilling work parts, their quality and installation operation specifications determine the drilling work Whether it can operate stably and with high quality. For the common ones at this stage Drilling tool failure accident analysis, constantly summarize its internal causes, accordingly Establish a sound drilling tool management system, on-site construction system, exploration injury system, etc., to reduce the occurrence of drilling tool failure as much as possible, fully enhance the international competitiveness of Global's energy industry.

REFRENCES

[1] Hui Quan, Jiayi Li, Jun Sun, et al.Gas-liquid separation mechanisms and bubble dynamics in a helical axial multiphase flow pump. Physics of Fluids 1 February 2025; 37(2): 023334.

[2] Johancsik C A, Friesen D B, Dawson R. Torque and drag in directional wells-prediction and measurement. Journal of Petroleum Technology, 1984, 36(6):987-992.

[3] Ho H S. An improved modeling program for computing the torque and drag in directional and deep wells. SPE 18047, 1998, 10.

[4] Gao D L, Liu F W, Xu B Y. Study on the buckling behavior of tubular columns in curved boreholes. Oil Drilling&ProductionTechnology, 2000, 22(4):1-4.

[5] Yang Y K, Jiang H W, Yuan Z P. Analysis and Research on downhole drill string coupling dynamics of extended reach wells. Drilling & Production Technology, 2018, 41(5):1-4+7.

[6] Wang Y H. Analysis and research of horizontal well completion string drivability. China University of Petroleum, 2008.

[7] Yu C L, Jin Y H. Friction prediction model establishment and running performance analysis of horizontal well completion string. China Petroleum Machinery, 2009, 37 (9):133-135.

[8] Hou S G, Yang Z H, Li B M, et al. Structural design and numerical simulation of windowed bit for ultra short radius horizontal wells. Drilling & Production Technology, 2014, 37(5):78-81.

[9] Zhang Y, Liu X M, Hua Z J, et al. Status and development trend of ultra short radius drilling technology. Drilling& Production Technology, 2023, 46 (2):41-45.

[10] Ma Z P. Research on prediction technology of friction, torque and casing wear in extended reach drilling. Northeast Petroleum University, 2015.

[11] Meng X W. Experimental study on friction torque of string in 3D curved borehole. China University of Petroleum (East China), 2017.

[12] Wang Z. Vibration mechanics and multiaxial stress strength analysis of mixed sucker rod string in curved wellbore. Yanshan University, 2022.

[13] Liu W J. Impact of drill string impact and wellbore internal pressure on wellbore stability. Southwest Petroleum University, 2014.

[14] Shi P, Wang J W, Liu X L. Nonlinear dynamic simulation analysis of drilling tool coal and rock based on ABAQUS. Journal of Dalian University, 2015, 36(3):32-35.

[15] Zhang Z, Ren W, Shi C, et al. Review on the Underbalanced Drilling Technology in Petroleum Industry. Journal of Research in Science and Engineering, 2021.

[16] Zhang L, Jin Y, Ma L, et al. Research on the treatment and secondary fluid mixing technology for oil-containing drilling wastewater in gas fields. Desalination and Water Treatment, 2024, 320100855-100855.

[17] Fan L, Deng L. Research on Optimization and Innovation of Oil Drilling Technology based on Cost Control Perspective. Journal of Innovation and Development, 2024, 7(2):15-18.

[18] Flik E A, Tyaglivaya I N, Zhukova I Y. Safe Technologies in the Oil Industry: Opportunities and Prospects for the Use of Polysaccharide Structure-Forming Agents in Drilling Fluids. IOP Conference Series: Earth and Environmental Science, 2021, 666 (2): 022062.

[19] Hai W, He Y, Li Y, et al. Multi-element drilling parameter optimization based on drillstring dynamics and ROP model. Geoenergy Science and Engineering, 2025, 244213460-213460.

[20] Jiangang W, Lei S, Ding F, et al. A digital twin modeling and application for gear rack drilling rigs lifting system. Scientific Reports, 2024, 14 (1): 23711-23711.

[21] Jing Y, Bo Z, Pingliang F, et al. Current Status and Trends in Shale Oil and Gas Drilling Engineering Technology Development at Home and Abroad. Journal of Physics: Conference Series, 2024, 2834 (1):012174-012174.